

Supporting Information:

Enhanced antimicrobial activity and structural transitions of a nanofibrillated cellulose-nisin bio-composite suspension

Ramon Weishaupt[†], Lukas Heuberger[†], Gilberto Siqueira[§], Beatrice Gutt[†], Tanja Zimmermann[§], Katharina Maniura-Weber[†], Stefan Salentinig^{†,}, Greta Faccio^{†,*}*

[†] Laboratory for Biointerfaces, Empa, Swiss Federal Laboratories for Materials Science and Technology, Lerchenfeldstrasse 5, CH-9014, St. Gallen, Switzerland

[§] Laboratory for Applied Wood Materials, Empa, Swiss Federal Laboratories for Materials Science and Technology, Überlandstrasse 129, CH-8600, Dübendorf, Switzerland

*greta.faccio@gmail.com,*stefan.salentinig@empa.ch

BCA peptide quantification assay. The nisin concentration in the washed TONFC-nisin biocomposite suspensions was measured as changes in absorbance (n=6) relative to polypeptide references (BSA, Bovine Serum Albumin) of known concentrations. The determined nisin concentrations were then normalized by the final TONFC concentration. Bare TONFC suspension at identical concentrations and treated accordingly was used as background.

Interfering signals potentially deriving from the presence of TONFC suspension during the BCA-peptide quantification assay were analyzed. A reaction mixture containing 0.364 $\mu\text{g/mL}$ nisin and 0.24 mg bare TONFC/mL prepared in 20 mM McIlvaine adhesion buffer, pH 5.8 was prepared, incubated at 160 rpm, and RT for 3 hours. The mixture was then centrifuged ($20'000 \times g$, 3 min), washed 2-times in equal volume of fresh adhesion buffer, resuspended thoroughly by pipetting, followed by ultrasonic treatment in a water bath (Branson 52, Branson Ultrasonics SA, Carouge-CH). Samples from different steps during the preparation were taken and analyzed for nisin content using the BCA-quantification assay. Indirect quantification of adsorbing peptide was done by subtracting the amount of peptide remaining in the supernatant after centrifugation ($14'000 \times g$) from the total amount of peptide (initially) in the initial solution. The resulting difference (ΔC) was normalized by the administered TONFC content (indirect). Statistical analysis was done using the statistical analysis tools of the PrismTM software (Version 6.07, June 12, 2015, Graphpad Software Inc. San Diego CA-USA).

SDS PAGE analysis. Gel electrophoresis (**Figure S1, C**) analysis was used to visualize purity of nisin solutions and the accumulation of monomeric nisin molecules (MW = 3354 Da) within TONFC materials after physisorption for 3 hours at RT in 20 mM McIlvaine¹ buffer at pH 5.8. 10 μL of solutions/suspensions containing 2.5 μg nisin were mixed with 20 μL of SDS PAGE loading buffer, denatured for 10 min at 95 °C and 15 μL applied to an 18% polyacrylamide gel. The gel was first rinsed in nanopure water twice for 10 min and secondly,

stained for polypeptides using the Pierce™ silver stain kit (Cat. no. 24612, ThermoFischerScientific, Waltham, MA-USA) according to the manufacturer’s instructions. The apparent size of the peptide was determined by comparing to the molecular weight standards (lane M) “Spectra Multicolor Low Range” (26628, ThermoFischerScientific, Waltham, MA-USA).

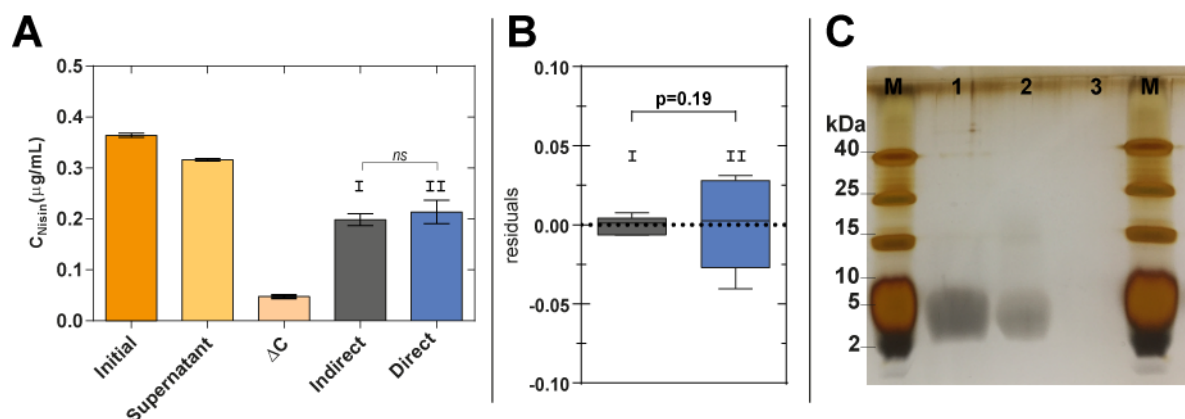


Figure S1. (A) Validation of direct quantification method of nisin from TONFC-nisin biocomposite suspensions. Values in graphs represent mean \pm standard deviation ($n \geq 3$). (B) Statistical validation of the peptide quantification assay in the presence of TONFC suspensions. The BCA assay signal of a TONFC-nisin biocomposite suspension (II) was compared to a nisin reference solution (I) containing identical amounts of peptide. The y-axis shows the residuals of a two-tailed t-test with Welch’s correction ($p \leq 0.05$). Boxes and whiskers represent 5-95 % percentiles of an unpaired t-test. (C) SDS PAGE analysis of 2.5 μg nisin (M_w 3’354 Da) fractions in solution (lane 1), immobilized to TONFC, after repeated washing of the biocomposite suspension with buffer (lane 2), and equivalent amount of untreated TONFC (lane 3). All samples were prepared at pH 5.8 and 20 mM ionic strength conditions. The molecular weight standards are reported in kDa (lane M)

Figure S1 (A) the validation of the BCA assay for quantification of nisin from TONFC-nisin suspensions. Statistical analysis revealed no significant difference between indirect quantification of nisin from the supernatant of biocomposite suspensions (I) and direct quanti-

fication of nisin from TONFC-nisin suspensions (II), despite the higher variance measured for TONFC-containing samples (Figure S1, B). These results validated the BCA-quantification assay to be applicable for direct quantification of nisin immobilized to TONFC suspensions *via* physical interactions. Based on these tests, a minimum of 6 replicates were used for quantitative results for TONFC containing samples. Additionally, qualitative analysis using SDS PAGE (**Figure S1, C**) verified purity and the monomeric state of soluble nisin (lane 1) and TONFC immobilized nisin (lane 2).

Physical characterization of TONFC-nisin interaction

Table S1. ζ potential measurement of pristine TONFC and TONFC-nisin biocomposite.

pH ^a	ζ potential (mV) ^b	
	TONFC	TONFC-nisin
2.0	-7.51±3.36	0.63±1.48
3.8	-33.88±2.28	-17.3±3.13
5.8	-37.75±2.64	-41.57±3.92
8.0	-42.23±3.80	-50.23±4.10
9.5	-46.65±5.17	-37.45±5.99

^apH of defined buffer at an ionic strength of 20 mM which was used to measure pH dependent ζ potential of TONFC samples, ^bAverage ζ potential measured in mV \pm standard deviation. Values are reported as average \pm standard deviation (n \geq 6).

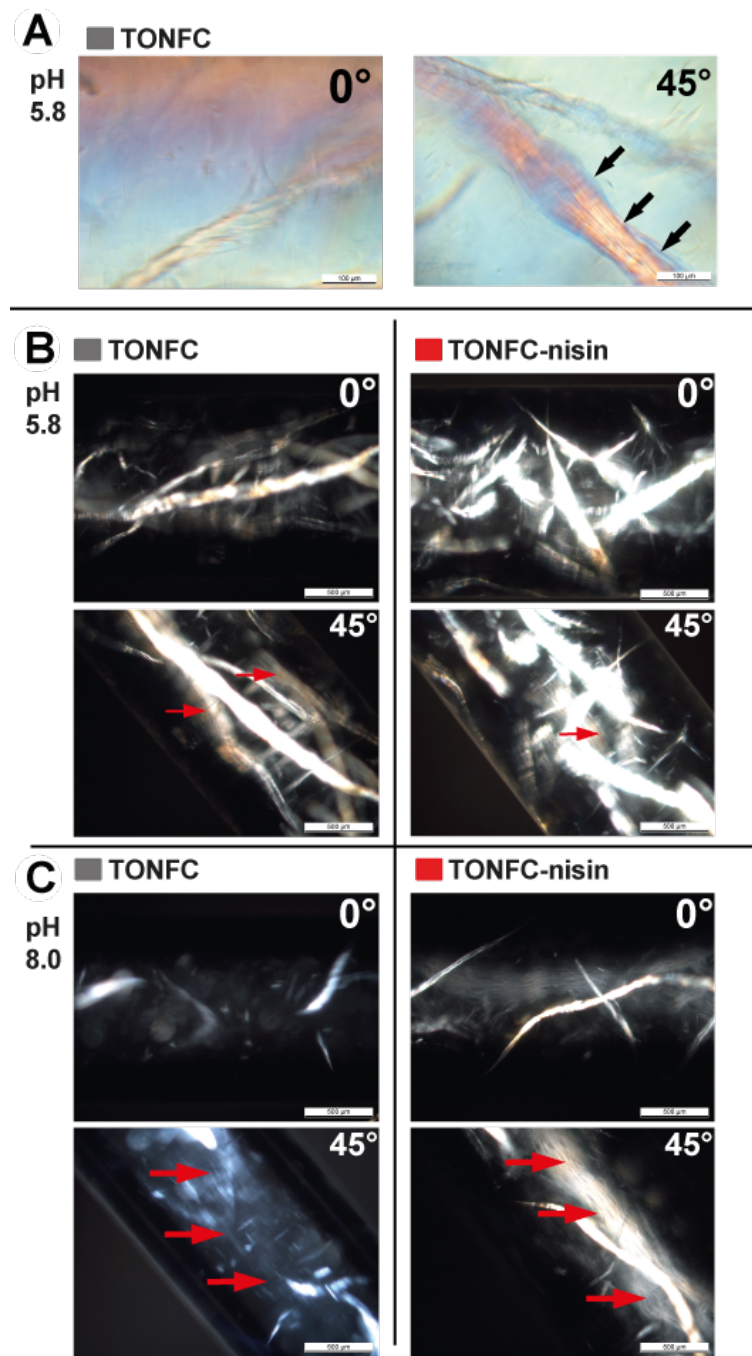


Figure S2. Optical microscopy images in cross-polarized light mode (transmission) of SAXS capillaries filled with bare TONFC (grey) and TONFC-nisin suspension (red) containing 0.4 % w/v TONFC at pH 5.8 (A) and pH 8.0 (B) taken at (left) 0°, (right) 45. Scale bars: 500 μm (left). Higher resolution image of bare TONFC at pH 5.8 taken at (left) 0°, (right) 45. Scale bars: 100 μm (C).

At the OM images at 45°, angle corresponding to maximal transmittance, some regions in the capillaries (indicated by arrows) become brighter, and this effect is ascribed to enhanced light scattering by more oriented cellulose fibril bundles inside the SAXS capillaries.

Calculation of the specific surface area of the TONFC fibrils in suspension

The specific surface area (SSA) is calculated as described elsewhere,^{2,3} using equation S1:

$$SSA = \frac{4}{d \cdot \rho} \quad (S1)$$

The density of cellulose⁴ ρ is $1.5 \cdot 10^6$ g/m³ and $d(m)$ is the average fibril diameter in meters calculated using equation S2:

$$d(m) = \frac{2r(nm)}{\sqrt{a}} * 10^{-9} \quad (S2)$$

r is the radius in nanometer and a is the axis ratio obtained by the dimensional reconstruction from the SAXS measurements (assuming a cylinder).

Based on the determined dimensional parameters (**Table 1**) and equations S1 & S2 a specific surface area (SSA) of 454 m²/g (pH 5.8) and 890 m²/g (pH 8.0) could be calculated for bare TONFC in suspension. Previously an SSA of 240 m²/g of TONFC study derived from the identical batch was calculated using the BET method.³ Although the SSA values obtained by both measurements were in a comparable range, the 1.9 - 3.8-fold lower SSA previously measured was most likely due to minor aggregation of fibrils that could occur during the sample preparation process (critical point drying) while the SSA values in this study were obtained for a never-dried, aqueous TONFC suspension.

Antimicrobial testing using the engineered *B. subtilis* bio-reporter strain

In particular, the *B. subtilis* bio-reporter strain sensed how effectively the TONFC-immobilized nisin molecules were translocated to specific bacterial cell surface moieties such

as the primary bacterial cell envelope lipid II target domains.⁵ The engineered bacterial stress-sensing two-component system PsdRS induces the transcription of ABC efflux transporter proteins which in turn remove the antibacterial agents from the cell.⁶

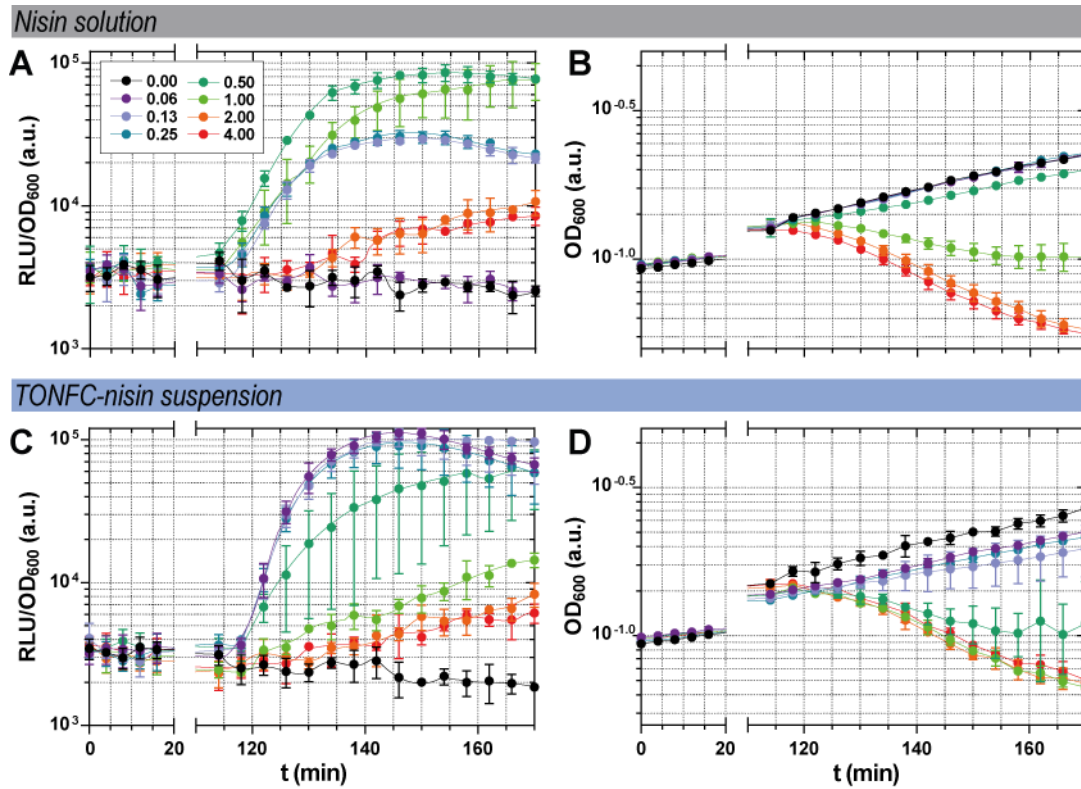


Figure S3. Time-resolved measurement of the bio-reporter strain *B. subtilis* PpsdA promoter activities exposed to increasing concentrations of soluble nisin (A) and TONFC-nisin suspension, grown in 120 mM LBM9 medium at pH 7.0 (C). The corresponding growth curves of the reporter strain grown in the presence of increasing concentrations of soluble nisin (B) and TONFC-nisin suspensions (D). The relative luminescence signals (RLU) are normalized by growth (OD_{600}). Graphs A-D show mean values and standard deviations ($n \geq 3$).

Antimicrobial testing against pathogenic *Staphylococcus aureus* model strain.

The non-inhibitory concentration “NIC” is defined according to Lambert and Pearson ⁹, as the line tangential to the point ($c[\log IC_{50}], y(c)$) respectively calculated according to Equation S4:

$$NIC [\mu g/mL] = 10^{\frac{1}{2b}(a+d)+c} \quad (S3)$$

For each tested condition, at least four measurements were performed derived from two independent experiments and obtained results collected in Table S2 and plotted in **Figure S4**.

Table S2. Parameters of the 4-PLS sigmoidal dose response curve fits.

Conditions/ Values	LB-M9		TrisHCl	
	Soluble nisin	Biocomposite	Soluble nisin	Biocomposite
Top ^a	0.85	0.93	1.00	0.93
Bottom ^b	0	0	0	0
LogIC ₅₀ ^c	0.81	0.44	-0.85	-0.27
HillSlope ^d	-14.06	-6.35	-1.73	-7.50
DOF ^e	81	82	45	42
R ^{2f}	0.92	0.97	0.96	0.97

^aTop limit of growth yield (FA) relative to reference samples containing bare TONFC (biocomposite) at the highest tested concentration or equal amounts of buffer (soluble nisin), ^bLower limit of growth yield (FA) corresponding to complete inhibition of growth over 24 hours of testing, ^cLogarithm of the inhibitory concentration ($\mu g/mL$ nisin) reducing growth yield to 50% relative to maximum growth, ^dHill slope describes the steepness of the curve, ^edegree of freedom, ^fGoodness of fit.

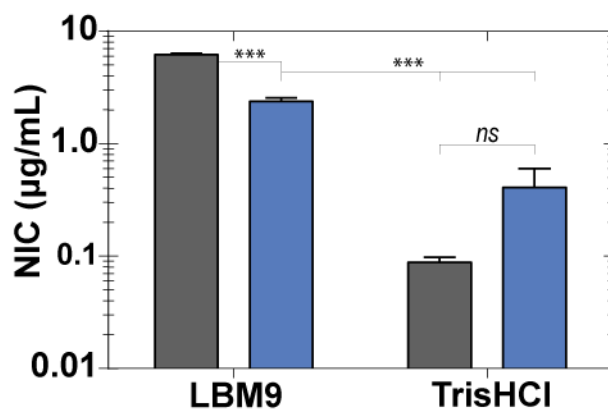


Figure S4. Calculated non-inhibitory concentrations (NIC) needed to induce a minimal level of *S. aureus* test strain growth inhibition. Values in graphs represent mean \pm standard deviation for experiments in LBM9 medium ($n \geq 8$) and Tris-HCl buffer ($n \geq 4$). ($***P < 0.001$, $*P < 0.01$, ns = not significant).

Characterization of the TONFC-fibril network properties

SEM (scanning electron microscopy) imaging

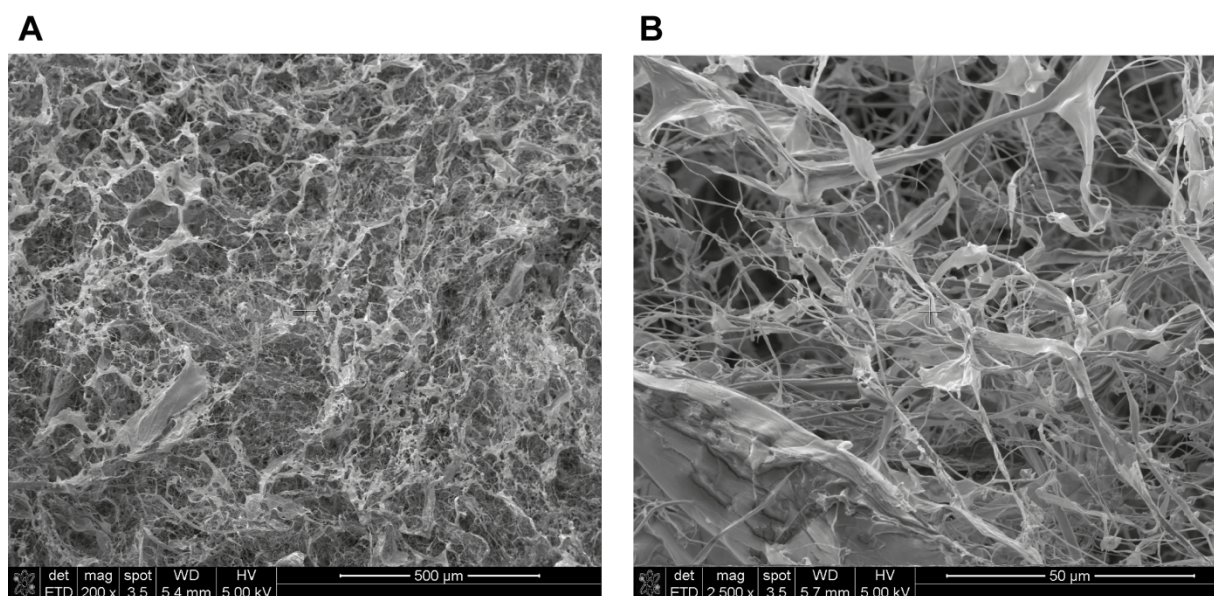


Figure S5. Representative SEM images of TONFC-fibril network structures prepared by freeze-drying at (A) 200-fold and (B) 2'500-fold magnification.

The apparent increase in average fibril diameter observed by SEM-imaging (**Figure 4 and Figure S5**) as compared to previously determined dimensional parameters by SAXS-measurements (**Table 1 & Scheme 2**) might be related to fibril aggregation during sample preparation (SEM) as the network properties can markedly differ between those that were never-dried (SAXS) and those that have been in a dried state (SEM).¹⁰



Figure S6. Representative SEM image of *S. aureus* test strain cultures incubated in sole buffer in absence of nisin freeze-at 50'000-fold magnification.

The strain culture grown in absence of nisin (**Figure S6**) developed round micro colonies with round shaped morphologies indicating viable bacterial cells with an intact cell envelope.

References

1. McIlvaine, T. C., A buffer solution for colorimetric comparison. *J. Biol. Chem.* **1921**, *49* (1), 183-186.
2. Sehaqui, H.; Zhou, Q.; Ikkala, O.; Berglund, L. A., Strong and Tough Cellulose Nanopaper with High Specific Surface Area and Porosity. *Biomacromolecules* **2011**, *12* (10), 3638-3644.
3. Weishaupt, R.; Siqueira, G.; Schubert, M.; Tingaut, P.; Maniura-Weber, K.; Zimmermann, T.; Thöny-Meyer, L.; Faccio, G.; Ihssen, J., TEMPO-Oxidized Nanofibrillated Cellulose as a High Density Carrier for Bioactive Molecules. *Biomacromolecules* **2015**, *16* (11), 3640–3650.
4. Sehaqui, H.; Zhou, Q.; Berglund, L. A., High-porosity aerogels of high specific surface area prepared from nanofibrillated cellulose (NFC). *Compos. Sci. Technol.* **2011**, *71* (13), 1593-1599.
5. Hsu, S.-T. D.; Breukink, E.; Tischenko, E.; Lutters, M. A. G.; de Kruijff, B.; Kaptein, R.; Bonvin, A. M. J. J.; van Nuland, N. A. J., The nisin-lipid II complex reveals a pyrophosphate cage that provides a blueprint for novel antibiotics. *Nat. Struct. Mol. Biol.* **2004**, *11* (10), 963-967.
6. Staroń, A.; Finkeisen, D. E.; Mascher, T., Peptide antibiotic sensing and detoxification modules of *Bacillus subtilis*. *Antimicrob. Agents Chemother.* **2011**, *55* (2), 515-525.
7. Radeck, J.; Kraft, K.; Bartels, J.; Cikovic, T.; Dürr, F.; Emenegger, J.; Kelterborn, S.; Sauer, C.; Fritz, G.; Gebhard, S.; Mascher, T., The *Bacillus* BioBrick Box: generation and evaluation of essential genetic building blocks for standardized work with *Bacillus subtilis*. *J. Biol. Eng.* **2013**, *7* (1), 1-17.

8. DeLean, A.; Munson, P.; Rodbard, D., Simultaneous analysis of families of sigmoidal curves: application to bioassay, radioligand assay, and physiological dose-response curves. *Am. J. Physiol.: Gastrointest. Liver Physiol.* **1978**, *235* (2), G97-102.
9. Lambert, R. J. W.; Pearson, J., Susceptibility testing: accurate and reproducible minimum inhibitory concentration (MIC) and non-inhibitory concentration (NIC) values. *J. Appl. Microbiol.* **2000**, *88* (5), 784-790.
10. Clasen, C.; Sultanova, B.; Wilhelms, T.; Heisig, P.; Kulicke, W. M., Effects of Different Drying Processes on the Material Properties of Bacterial Cellulose Membranes. *Macromolecular Symposia* **2006**, *244* (1), 48-58.